香港天文台
HONG KONG OBSERVATORY

Reprint 640

Three-dimensional Surface Cracking and Faulting in Dangan Islands Area, South of Hong Kong

K.T. Chau [1], R.H.C. Wong [1], Y.L.Wong [1], K.W. Lai [1], L.X. Wang [1], Y.W. Chan, W.T. Wong, Y.S.H. Guo [2], W. Zhu [2] & S.H. Zheng [3]

3rd International Conference on Continental Earthquakes, Beijing, China, 12-14 July 2004

[1] *Department of Civil & Structural Engineering, The Hong Kong Polytechnic University*

[2] *Geotechnical and Structural Engineering Research Center, Shandong University*

[3] *Center for Analysis and Prediction, China Earthquake Administration*

THREE-DIMENSIONAL SURFACE CRACKING AND FAULTING IN DANGAN ISLANDS AREA, SOUTH OF HONG KONG

K.T. Chau[1], R.H.C. Wong[1], Y.L.Wong[1], K.W. Lai[1], L.X. Wang[1], Y.W. Chan[2], W.T. Wong [2], Y.S.H. Guo[3], W. Zhu[3], and S.H. Zheng[4]

[1]Department of Civil & Structural Engineering, The Hong Kong Polytechnic University, Kowloon, Hong Kong, China
[2]Hong Kong Observatory, 134A Nathan Road, Kowloon, Hong Kong, China
[3]Geotechnical and Structural Engineering Research Center, Shandong University, Jinan, Shandong, China
[4]Center for Analysis and Prediction, China Earthquake Administration, No. 63 Fuxing Avenue, Beijing, China

ABSTRACT

On June 23, 1874, an earthquake of magnitude $5^3/_4$ occurred about 11 km northeast of Dangan Main Island, and the epicenter was around 30km southeast from Tsimshatsui of Hong Kong. Chinese seismologists estimated that the maximum credible earthquake magnitude from this potential seismic source is up to 7 or 7.5. Therefore, this paper summarizes our recent studies in fault zone mapping of the Dangan Islands by field excursions, earthquake data analyses, and experimental and theoretical studies on three-dimensional surface cracking. In particular, the foci of a total of 26 small earthquakes within 150 km of Hong Kong recorded by the Hong Kong Observatory since 1998 are plotted three-dimensionally, and 3 potential fault zones are identified. Fault zones on Dangan Island are identified from our field excursions to the island, and a series of normal faults trending ESE and NE were found on the island. To examine the potential future faulting, specimens containing 3-D surface cracks are compressed to examine the cracking pattern. Shell and pedal cracks around the pre-existing three-dimensional surface crack were observed. Theoretical crack models and stress singularities at the intersection between the surface crack and the free surface are investigated. A new formula is proposed to estimate the wing crack length as a function of applied stress, crack inclination, Poisson's ratio, and fracture toughness. The results of this study should lead to better understanding of future continental earthquakes occurring from surface faults.

1. INTRODUCTION

Seismologically, Dangan Islands are located near the Binhai Fracture zone at the northern part of the South China Sea, which separates the continental shelf of southern China and the depressed basin in the South China Sea. The thickness of the Earth's crust changes abruptly across the Dangan Islands area (Xia, 1985). On June 23, 1874, an earthquake of magnitude $5^3/_4$ occurred about 11 km northeast of Dangan Main Island. The earthquake led to a felt earth tremor in Hong Kong of intensity VI on the Modified Mercalli scale. This is the largest earthquake occurred within 35 km of Hong Kong in the past 500 years. According to the Daily Press, the ground shaking was felt along the NE-SW direction. Some people were injured while two houses collapsed, boulders were dislodged from slopes and some retaining walls collapsed. There were also observable ground waves, bells rang and water in the harbour was "rough and buoyant" (Lee and Workman, 1996). Thus, Dangan Islands area is definitely a potential seismic source that is capable of generating large earthquakes affecting Hong Kong. Figure 1 shows satellite photograph of the Hong Kong Island and Dangan Islands.

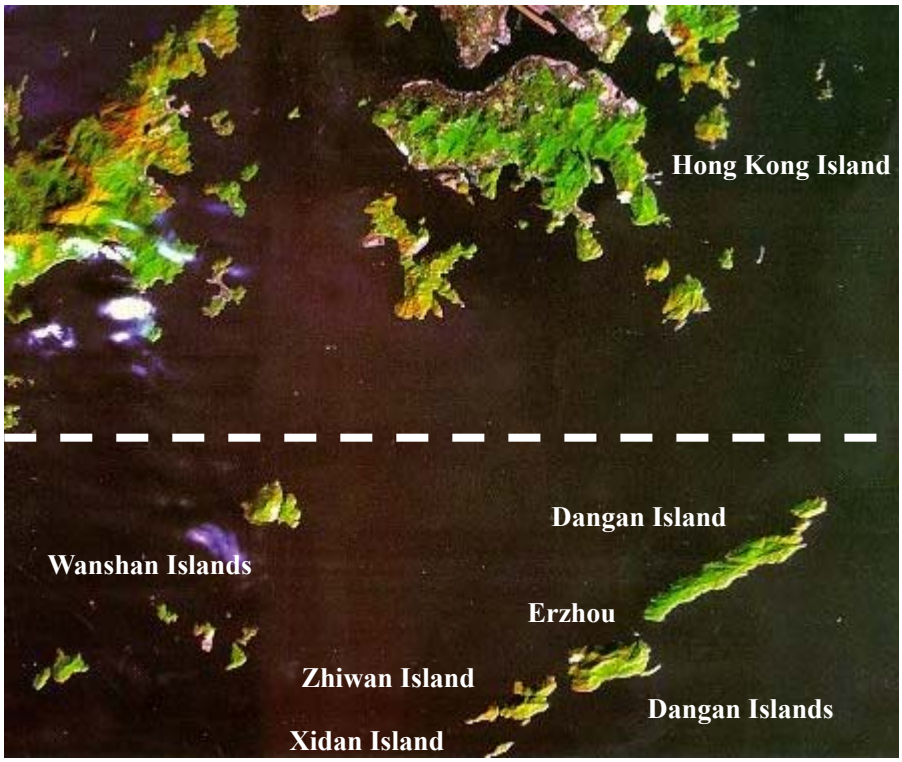

Figure 1. The location of Dangan Islands and Hong Kong, and the dotted white line is southern boundary of Hong Kong waters with all islands south of is under the administration of Zuhai

A closer look of the geological setting in South China reveals that there is a large fault system in the northern South China Sea. This fracture zone is called "Binhai Fracture Zone" or "Littoral Fault Zone". A major earthquake occurred along this fracture zone was the 1918 Shantou earthquake of magnitude 7.3 and the epicentre was located about 340km east-northeast of Hong Kong; and there was also the 1605 Qiongshan earthquake of magnitude 7.5 about 450 km to the west of Hong Kong (Feng, 1988). There is, however, a "large-earthquake-missing-zone" in the middle around Hong Kong. The geological setting of this section of "Binhai Fracture Zone" is similar to those observed at both Shantou and Qionshan areas; therefore, it is commonly believed by seismologists that this section of fault zone near Dangan Island is also capable of producing destructive earthquakes of magnitude up to 7 or 7.5.

Therefore, in view of the 1874 earthquake and in view of the potential of producing an earthquake of 7 to 7.5 in Dangan Islands area, the study of the fault zones in Dangan Island and nearby waters is of particular relevance to Hong Kong. In this paper, we will first analyze the small earthquake data in the Dangan Islands area recorded by the Hong Kong Observatory in Section 2. The potential sub-surface fault geometry will be inferred from earthquake data. Section 3 will summarize the finding of our geological excursions to Dangan Island. Section 4 continues to present some of our recent experiments on 3-D surface cracking. The patterns of crack growth from a pre-existing 3-D surface crack will be summarized. Section 5 will discuss some of the theoretical results from fracture mechanics and their implication to our experiments and to the faulting problem in northern part of South China Sea, before the conclusions are made in Section 6.

2. EARTHQUAKE DATA ANALYSES FOR DANGAN ISLANDS AREA

In order to examine the sub-surface faulting pattern in Dangan Islands area, we propose to plot the foci of small earthquakes recorded by the Hong Kong Observatory with latitude of 21.0-22.5N and longitude of 113.5-115.5E. Therefore, as a preliminary analysis, the foci of a total of 26 small earthquakes recorded by the Hong Kong Observatory since 1998 are plotted three-dimensionally in Figure 2. The magnitude of these earthquakes range from 1.6 to 3.2, whereas the depth of these foci ranges from 0 to 59 km (all shallow earthquakes).

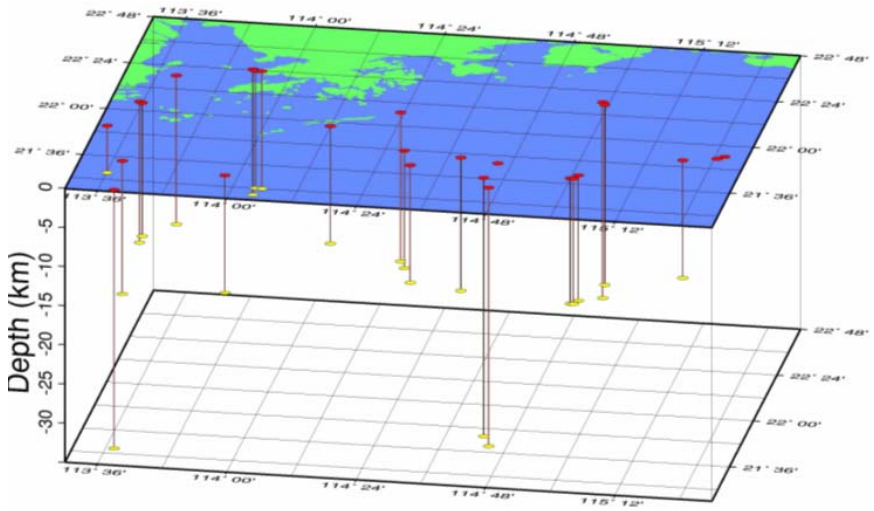

Figure 2. Locations of the 26 earthquake data for three-dimensional analysis

Using software capable of showing three-dimensional plots, we can search for any common plane that some of these data may fall onto. These common planes may indicate both dip angle and strike directions of "active" fault planes (active in the sense that small earthquakes are constantly generated on these fault planes). These planes, once identified, may be identified as potential fault planes for generating further probable "large events". With this objective in mind, three potential faults were identified after viewing the data along all possible perspective angles of observation (see Figure 3). There are about 7, 8 and 6 data lies onto these three-dimensional surfaces, labeled as Fault Planes 1-1, 2-2, and 3-3. The corresponding dip direction/dip angle of these planes are 145°/40°, 45°/60° and 315°/70°. In addition, the surface outcrop of Fault Plane 1-1 may appear at parts of Hong Kong. However, no distinct fault zone was found on the projected surface (Lai and Lanford, 1996). Therefore, we infer that Fault Plane 1-1 may curve up as shown in Figure 3 (see the "question mark").

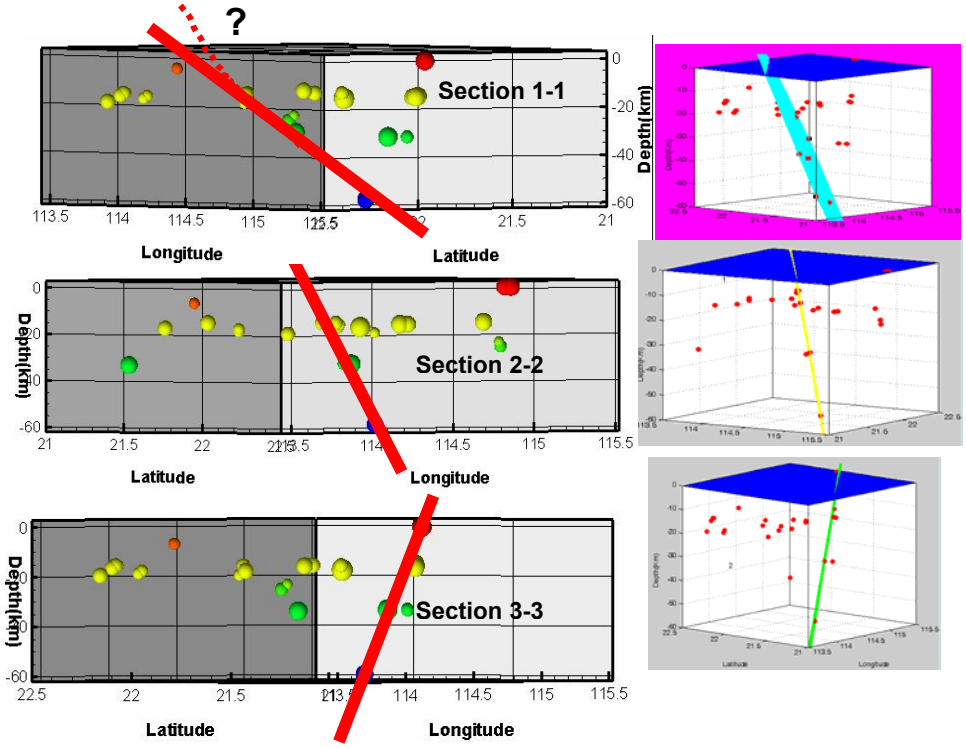

Figure 3. Three-dimensional identification of potential fault lines based on earthquake data

The three dimensional plots of these fault planes are shown in Figure 4(a) together with a plan view showing the possible outcrops of these fault planes in Figure 4(b).

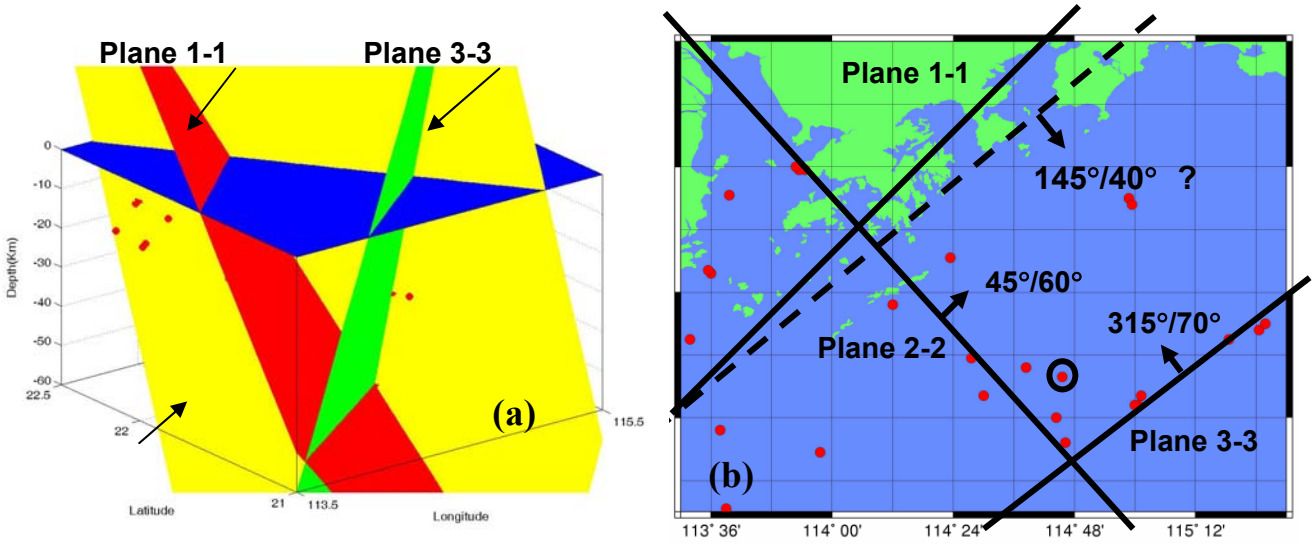

Figure 4. (a) Three-dimensional plot of the three inferred fault planes; (b) Plane view of the outcrops of Fault Planes 1-1, 2-2, and 3-3.

The dotted Fault Plane 1-1, which is the adjusted surface outcrop of the Fault Plane 1-1 (see also the dotted line marked with “question mark” in Fig. 3), lies roughly on the so-called Haifeng Fault Zone.

Therefore, our interpretation is that some of these small earthquakes occurred in South China Sea close to Dangan Island may be associated with the Haifeng Fault Zone. This is, of course, a very preliminary interpretation, and further evidence is needed to verify this hypothesis. Additional analysis of small earthquake data recorded by the Hong Kong Observatory before 1998 would be useful to verify the results of the present study. It is of interest to point out that the earthquake data being "circled" in Figure 4(b) is at the intersecting point of all three interpreted fault planes.

3. GEOLOGICAL SETTING OF DANGAN ISLAND

There are four main islands of Dangan Islands, namely: Dangan Island, Erzhou, Zhiwan Island, and Xidan Island. The Chinese name for "Dangan Island" literally means a "long rod" for carrying heavy items on shoulder, which reflects the shape of Dangan Island (see the satellite photograph shown in Figure 1). The surface area of Dangan Island is about 24 km^2. The highest point on Dangan Island is 322 m above sea level. Politically, Dangan Island is under the administration of Zhuhai Special Economic Zone. Two separate field excursions were made to the main Dangan Island (one in January and one in May, 2004). The full details of these field excursions will not be given here due to space limitation. Full report on the geological setting of fault systems on Dangan Island will be published in our later papers. Only a very brief summary will be given here.

Fault zones on Dangan Island are identified after our field excursions to the island, suggesting a series of normal faults trending SE to ESE (≈195°) and NE (≈65°) on the island (see Figure 5). The bedrock on the island is mainly granite. Mylonite was found along Fault Line 1 on Figure 5, while fault gouge samples were obtained from a sea cave formed along Fault Line 3. This suggests that fault line trending ESE is of younger age comparing to the NE trending fault lines on Dangan Island. The outcrop of Fault Line 1 appears impressively as a high cliff of 129.8 m high (see Figure 6). The patterns of deformations on joint sets on both sides of the fault strongly suggest that it is a normal fault (as shown by arrows in Figure 6).

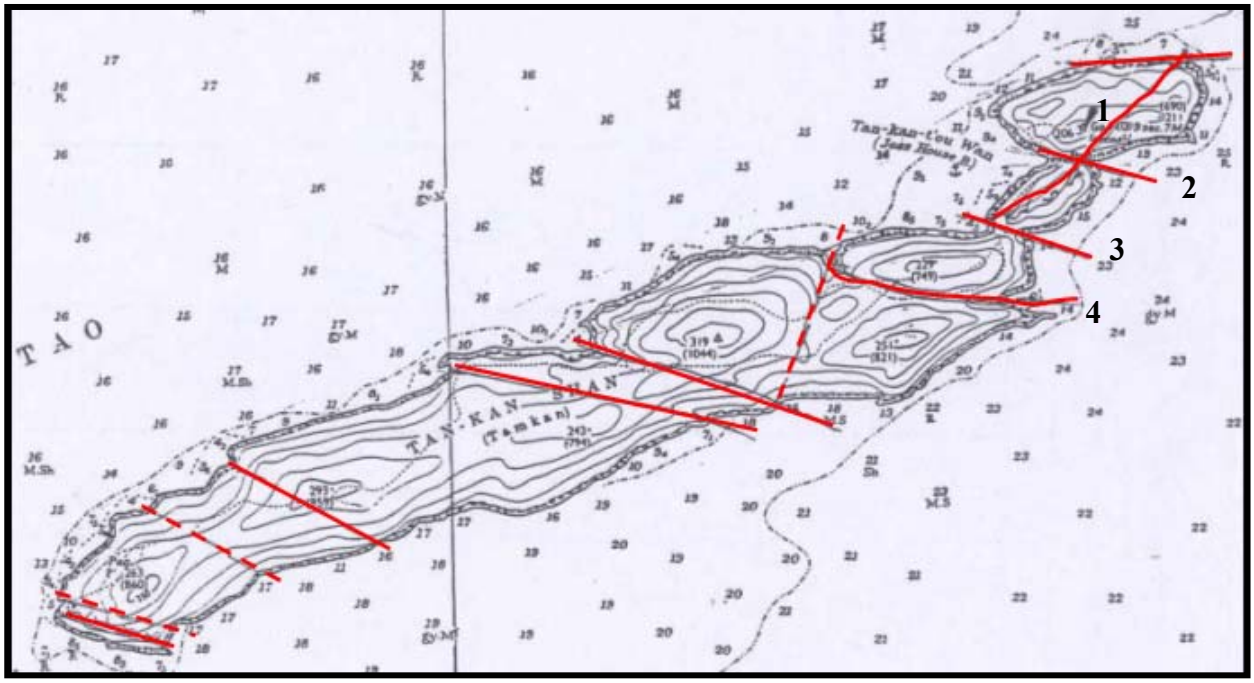

Figure 5. Fault lines observed or inferred from field excursions

Figure 6. A photograph of Fault Line 1 shown in Figure 4, which was taken at a location close to the intersection between Fault Lines 1 and 2

The Fault Line 4 shown in Figure 5 can be seen clearly from air (see Figure 7). The dip direction/dip angle of this Fault Line 4 is 190/70. The gouges sample obtained from a sea cave along Fault Line 3, which is shown in Figure 7(b), will be sent to Institute of Geology for determining the time of last active earthquake event. Using such method of dating, we should be able to assess the earthquake hazard induced by these faults.

At this moment, the fault zones identified in Section 2 from small earthquake data does not match exactly with the surface fault lines on Dangan Island that we observed from field excursions. Hopefully, after we obtained more earthquake data for the region before 1998, we should be able to identify any interplay between these surface faults and the sub-surface faults along which these small earthquakes were generated.

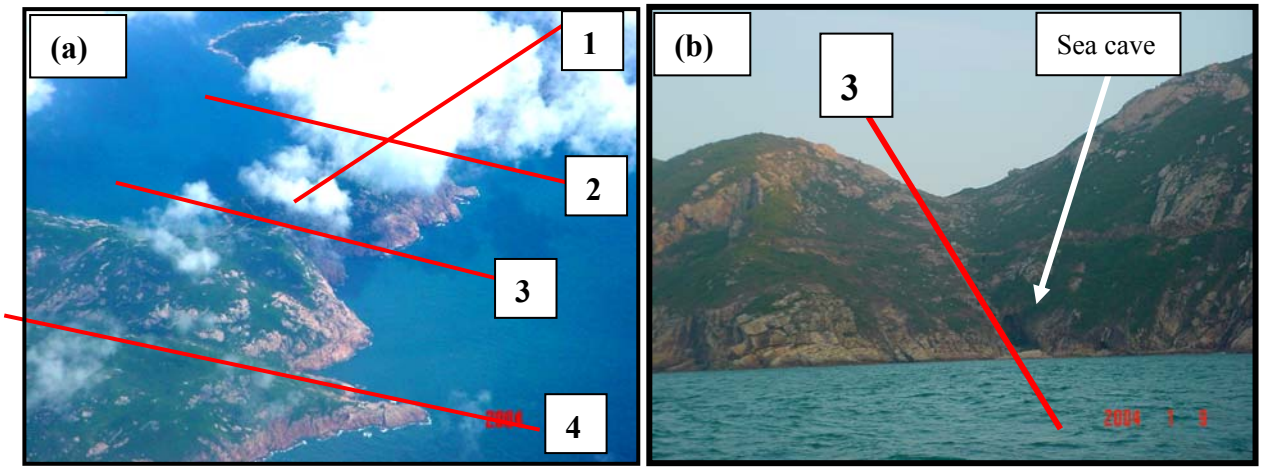

Figure 7. (a) A aerial photograph showing Fault Lines 1-4 shown in Figure 5; (b) the location of the sea cave found along Fault Line 3, at where fault gouge samples were taken

4. EXPERIMENTS ON THREE-DIMENSIONAL SURFACE CRACKS

Series of experiments on surface cracking have been conducted at the Hong Kong Polytechnic University (PolyU) and at Shandong University. Some of these results will be summarized here. For full details of the experiments conducted at PolyU, the readers should refer to Wong et al. (2004a-b).

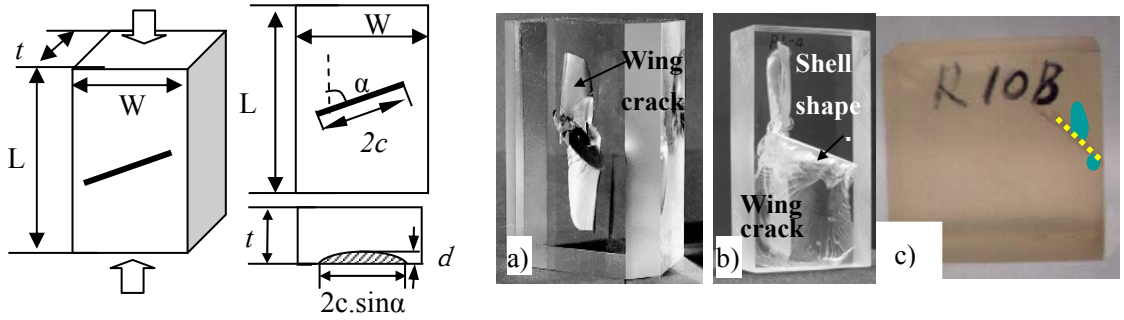

Figure 8. A sketch of our experimental set-up, and cracking in 3 different samples: (a) 3-D internal crack in PMMA (Dyskin et al., 1994); (b) 3-D surface crack in PMMA (Wong et al. 2004a); and (c) Resin specimen in Shandong University

Figure 8 sketches the layout of our tested samples and define the parameters defining the three -dimensional surface crack used in our experiments, together with the actual samples tested by Dyskin et al. (1994), by Wong et al. (2004a) at PolyU and by Guo and Zhu at Shandong University. The crack depth, crack length and crack angle are denoted by d, $2c$, and α respectively as shown in Figure 8. The height, width and thickness of the sample are denoted by L, W and t respectively. For those experiments conducted at PolyU, the crack depth to thickness ratio is within the following range: $0.66 > d/t \geq 0.21$. In our experiments, the crack is made by cutting a notch of circular shape on the sample (such crack is termed partially circular crack by Murakami and Natsume, 2002). In general, it is observed that crack propagation is much more vibrant for smaller d/t, as expected (see Wong et al., 2004a-b). This crack size effect is well-known in classical elastic fracture mechanics that the stress intensity factor increases with the crack size; thereby, a sample containing a larger crack is more conductive crack growth under compression than one containing a smaller crack (Broberg, 1999).

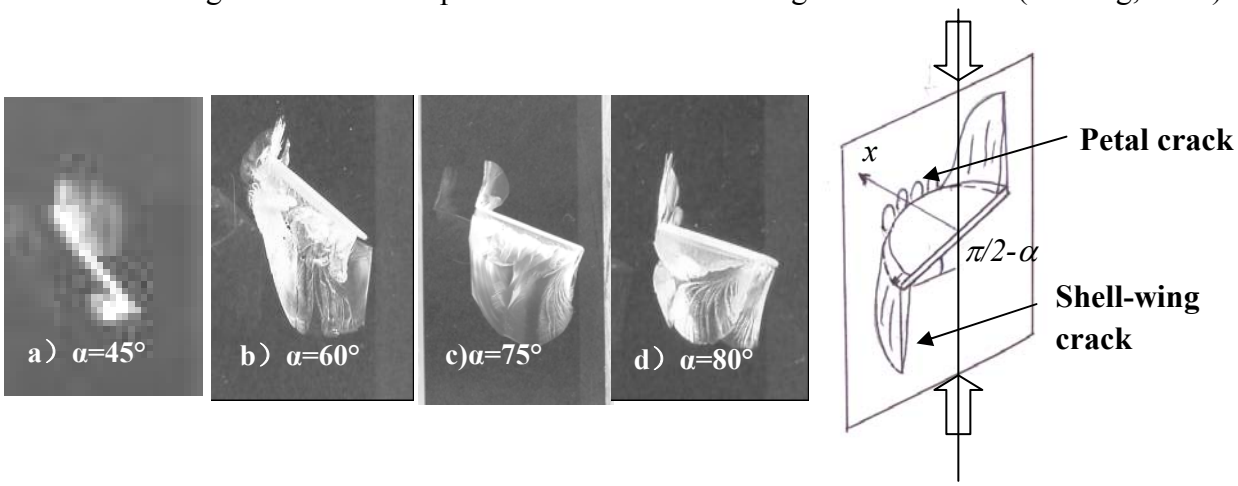

Figure 9. The growth of shell-wing crack, which a wing crack with a curvilinear surface, as a function of α (a-d). A schematic sketch showing mode III petal cracks and mode I wing cracks

For PMMA specimens, a series of experiments were conducted to investigate the mechanism of crack propagation for specimen containing a 3-D crack of varying α (15°, 30°, 45°, 60°, 75° and 80°). The results are shown in Figure 9. The crack length is fixed at $2c/w$=0.28 and the value of d/t of this group of specimens is 0.26, so that thickness effect is not significant. Experimental results show that for a specimen containing a crack with α of 15° or 30°, no crack growth is observed even when the specimen is stressed to yield. When α is larger or equals to 45°, initiation of wing cracks is observed. When α is larger or equal to 60° (see Fig. 9), both wing crack and petal cracks were nucleated from the pre-existing 3-D surface crack, and, since it not apparent from the figure, a sketch of these shell-wing crack and petal cracks is also given in Figure 9. When the load is large enough, these shell-shaped wing cracks did extend towards the free surface. Note, however that, the petal cracks do not appear when the specimen with the cutting flaw depth d/t< 0.25. Some preliminary experiments conducted at Shandong University also lead to similar conclusion.

Actually, real rock samples have been tested at PolyU. However, due to the non-transparent nature of rocks, three-dimensional development of cracking from the pre-existing surface crack cannot be observed and such results will not be discussed here (Wong et al. 2004a-b).

Although these three-dimensional surface cracks in our samples are highly simplified version of the actual surface fault that generating earthquakes, the crack growth mechanism observed in our laboratory may provide clues on how earthquake may happen in the earth crust. Much works remain to be done. For example, as shown in Sections 2 and 3 that real fault always intersect the free surface at certain dip angle (instead of vertical fault), especially for the case of normal faults. More experiments will be conducted on the effect of dip angle on surface cracking.

5. THEORETICAL ANALYSIS OF SURFACE CRACKS

5.1 *Vertex singularity*

There is a major difference between three-dimensional internal and surface cracks. It is a well-known result of linear elastic fracture mechanics that the stress near the crack tip exhibits a singularity of $r^{-0.5}$, where r is the distance measure from the crack tip (Borberg, 1999). However, it was proved by Benthem (1977, 1980) that this classical singularity does not hold at the edge of the crack at the free surface, but instead a singularity of the form r^{λ} exists. The singularity exponent λ is found to be a function of the mode of cracking (i.e. mode I, II or III), the inclination angle β of the crack front at the free surface, the inclination angle γ of the crack plane with the solid surface, and the Poisson's ratio of the solid. The definitions of these angles are given in Figure 10. The surface of the sample is denoted by the x-y surface, and the solid occupies $z \geq 0$. The outward normal direction of the free surface is denoted by $\boldsymbol{n}$ whereas the tangential vector on the plane of the three-dimensional crack is denoted by $\boldsymbol{s}$. In our experiments shown in Section 4, only the case of γ=0 have been tested. The thick arrows indicate the uniaxial compression, which forms an angle of α with the crack line on the free surface (i.e. the crack forms an angle of π/2−α with the x-axis).

Analytical results exist only for very special cases (β=π/2, γ=0), whereas most existing results were obtained through the use of very fine mesh finite element method, finite difference and hypersingular integral equation. Although the vertex singularity is of paramount importance in engineering application, these predictions of vertex singular component (or so-called Benthem singularity component) cannot be found on any handbook of stress intensity factors (e.g. Murakami, 1987; Tada et al., 1985). Therefore, there is a need to report these results here. Some approximate formulas are also proposed here for easy reference.

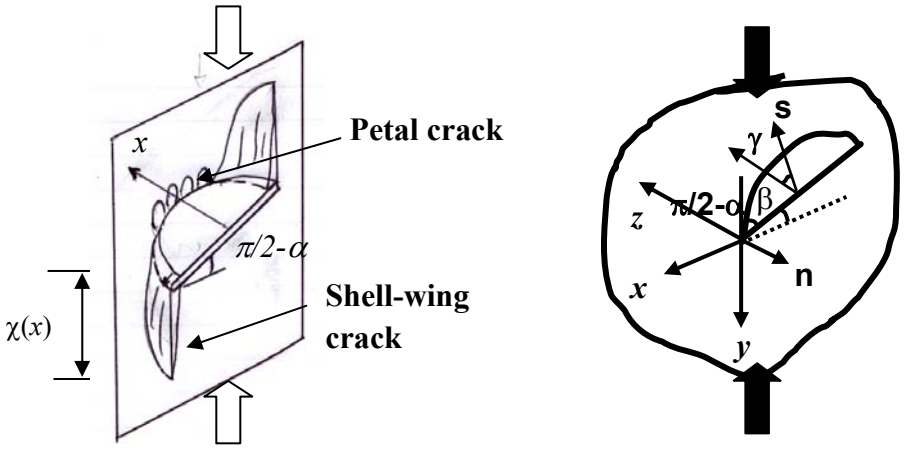

Figure 10. The geometry of a 3-D surface crack and cracking pattern of petal and wing cracks

In particular, the crack tip singular stresses are of the following form (for mode I, mode II and mode III respectively):

$$\sigma = \frac{K_I}{\sqrt{2\pi}} r^{\lambda} \quad , \quad \tau_{II} = \frac{K_{II}}{\sqrt{2\pi}} r^{\lambda} , \quad \tau_{III} = \frac{K_{III}}{\sqrt{2\pi}} r^{\lambda} \tag{5.1}$$

where σ, τ_{II}, and τ_{III} are the tensile stress, in-plane shear stress and anti-plane shear stress respectively. The exponent λ equals $-1/2$ if the crack tip is not close to the free surface. When the free surface is approached, the predominant (or called gravest) singularity component λ is given by both Benthem (1977) and Bazant and Estenssoro (1979). A simple curve fitting of their results lead to the following formula for the mode I with $\beta=\pi/2$ and $\gamma=0$:

$$\lambda = 14.049\nu^4 - 12.387\nu^4 + 4.4748\nu^3 - 0.4409\nu^2 + 0.1094\nu - 0.5 \tag{5.2}$$

with the coefficient of correlation of R^2=0.9999 and the predictions by (5.2) for all available data from Benthem (1977) and Bazant and Estenssoro (1979) are no worse than 0.3% error. For modes II and III cracks with $\beta=\pi/2$ and $\gamma=0$:

$$\lambda = 3.111\nu^4 - 2.882\nu^3 + 1.4911\nu^2 - 0.604\nu - 0.5 \tag{5.3}$$

with R^2=1 (i.e. a perfect of the data given by Bazant and Estenssoro, 1979). When the crack does not intersect the free surface at $\beta=\pi/2$, λ may be estimated from the following formula for the case of mode I with $\nu=0.3$ and $\gamma=0$:

$$\lambda = -0.2417\beta - 0.0731 \tag{5.4}$$

with the coefficient of correlation of R^2=0.9999 and β is in radian. These formulas of singularity exponents will be very useful if numerical method will be used further analyses. Note that equations (5.2)-(5.4) are originally proposed here and can be used easily by engineers and scientists.

5.2 *Stress intensity factor at the surface crack*

For the uniaxial compression adopted in our experiments, no solution is available in the literature for

the stress intensity factor around the 3-D partial circular crack. According to our experimental observation (given in Figure 9) the surface crack does propagate along the original crack plane, but rather wing tensile cracks nucleate from the upper and lower tips of the crack and petal cracks nucleate along an orthogonal direction. The far field compression can be dissolved into a shear stress component along the crack face and a normal compressive stress perpendicular to the crack face. The surface crack is produced by cutting a notch in the solid, so that the crack opening width is of the order of 1-2mm. It is very unlikely that compressive stress component is large enough to close the pre-existing crack faces and to induce frictional contact. The shear stress component appears to be large enough to wedge open the wing cracks at both tips, whereas the petal cracks (see Figure 9) along the internal edge of the cracks are clearly induced by mode III cracking (sliding along a direction normal to the crack front).

To interpret our experiment, we will first propose formulas of stress intensity factor for partially circular surface crack under far field shear stress (see Fig. 11).

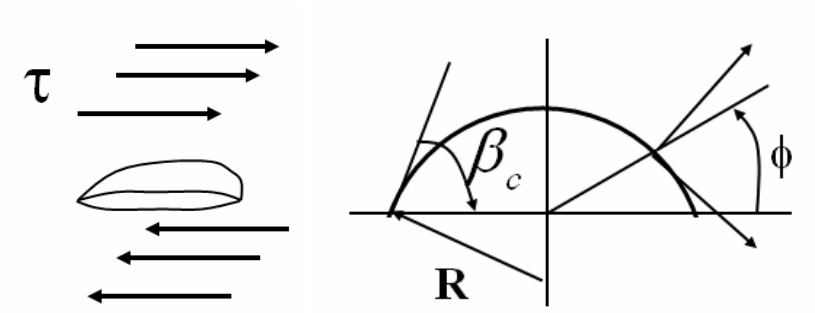

Figure 11. A partially circular crack subject to far field shear stress

The following formulas are obtained by fitting the data extracted from the numerical analysis by Murakami and Natsume (2002) for the of β_c=67° and ν=0.3 (this is the critical angle at the intersection of the crack and the free surface at which a classical singularity of λ=–0.5 is found, Bazant and Estenssoro, 1979). For mode II, stress intensity factor can be approximated by:

$$K_{II} = \tau\sqrt{\pi R}(-0.083\phi^4 + 0.4628\phi^3 - 0.8948\phi^2 + 0.3272\phi + 0.4055) \tag{5.5}$$

where ϕ is in degree and *R* is defined in Figure 11 (*R* equals 20mm in our experiments). The stress intensity factor for mode III is

$$K_{III} = \tau\sqrt{\pi R}(0.4169\phi^4 - 1.2983\phi^3 + 1.171\phi^2 - 0.1229\phi + 0.2809) \tag{5.6}$$

where ϕ is in degree. Although equations (5.5)-(5.6) are not exact, they are accurate enough for engineering applications.

As expected, K_{III} is at maximum when ϕ=π/2 and attains a minimum at ϕ=0. Therefore, mode III crack is likely to occur along the internal crack front as shown in Fig. 10. However, the observed petal cracks are orthogonal to the pre-existing crack face, instead of propagating along the pre-existing crack face. More theoretical work is needed to model the initiation as well as propagation of these petal cracks. On the other hand, K_{II} equals zero at ϕ=π/2 but the maximum does not attain at ϕ=0, but instead occurs at ϕ of about 0.03π to 0.1π. Note that because the surface crack is not orthogonal to

the free surface both mode II and III can be non-zero at the corner point of the crack (intersection of crack and free surface). This mode II shear sliding near the crack tips obviously wedge open a tensile wing crack as what we have observed in the experiments (see Figure 9). Both petal and wing cracks are results of crack branching phenomenon (i.e. crack propagates along a direction deviating from the original crack front). In addition, note also that the theoretical mode I stress intensity factor under this shear loading (see Figure 11) is zero; thus, an different model is needed to predict the wing crack propagation. A simple result of this kind is given in the next section.

5.3 *A simple model for wing crack*

The following model is modified from the wing crack model proposed by Dyskin et al. (1999) for an inclined penny-shaped crack (internal crack) under uniaxial compression. Due to symmetry, we can consider that an internal penny-shaped crack can be formed by putting two solids containing a three-dimensional half-circular surface crack together, with the surface crack line of each sample touching one another. If the crack movement is mainly sliding under far field compression (as what we observed in experiments), there should be no interaction between the two touching solids due to symmetry. Using this argument, the model by Dyskin et al. (1999) can easily be modified for our case of surface cracking. All we need to do is to modify the stress intensity factor from an internal penny-shaped crack case to that of a half-circular surface crack case.

It is well-known that the mode I and II stress intensity factors for a 2-D crack of size 2*a* subject to far stress can be used to find those for an edge crack (or surface crack) problem of crack size *a* subject to the same far field stress, simply by multiplying them with a factor of 1.1215 (while mode III remains the same) (e.g. Tada et al., 1985). However, such conversion factor is not well documented for the case of converting stress intensity factors of 3-D penny-shaped crack to those of half-circular surface crack. To find this, can first quote the mode II and III stress intensity factors for a penny-shaped crack of radius *a* subject to far shear stress τ (Tada et al., 1985):

$$K_{II}(\theta) = \frac{4\tau\cos\theta\sqrt{\pi a}}{\pi(2-\nu)}, \quad K_{III}(\theta) = -\frac{4(1-\nu)\tau\sin\theta\sqrt{\pi a}}{\pi(2-\nu)}, \tag{5.7}$$

where, as usual, ν is the Poisson's ratio and θ is the angle measured from the direction of the applied shear stress τ. The exact solution for a half-circular surface crack subject to far field stress τ is not available, but the numerical solutions reported by Murakami and Natsume (2002) can be used to estimate such factor. If we take the maximum K_{II} at θ=π/2 and maximum K_{III} at θ=0 from Murakami and Natsume (2002), we have the following conversion factor for both mode II and mode III:

$$R_{II}(\theta=\pi/2) = \frac{K_{II\max}^{surface}}{K_{II\max}^{penny}} \approx 1.7, \quad R_{III}(\theta=0) = \frac{K_{III\max}^{surface}}{K_{III\max}^{penny}} = 1 \tag{5.8}$$

where the superscripts "surface" and "penny" denote the value for surface crack and penny-shaped crack respectively. Actually, both R_{III} and R_{II} changes with orientation θ. But, the above formulae should consider the worst scenario since both maximum K_{II} and K_{III} have been considered.

With the help of these factors, we can modify the results by Dyskin et al. (1999) to yield the following formula for the wing crack length χ(*x*) as a function of uniaxial applied stress σ and others parameters of the solid:

$$\chi(x) = \frac{2b^2\sigma^2\left(\sin^2\alpha\cos\alpha\right)^2}{\pi(1-\nu)^2 K_{IC}^2}\left[1-\frac{x^2}{b^2}\right] \tag{5.9}$$

where

$$b = a\sqrt{(1-\frac{\tau_d^2}{\tau^2})}, \quad \tau_d = \frac{\sqrt{3}}{2} K_{IC} \frac{\pi(2-\nu)}{6.8\sqrt{\pi a}} \tag{5.10}$$

and K_{IC} is the mode I fracture toughness that can be found by standard experiments. The detailed arguments lead to derivation of (5.9) will not be given here due to space limitation. In this formula, α has the definition as defined in Figure 8. If we replace 6.8 by 4 in (5.10), the original formula by Dyskin et al. (1999) is recovered. It is straightforward to show that the wing crack propagation is in general longer than the case of internal penny-shaped crack. We must emphasize that this is only a preliminary model for the problem, and comprehensive calibration and comparison need to be done. Since the surface crack made is in our sample is in fact partially circular crack (instead of half-circular crack), the proposed model is only an approximation to the laboratory situation. Nevertheless, it should provide a good first order solution for the problem.

6. DISCUSSIONS AND CONCLUSIONS

In this paper, we have summarized our recent works on three-dimensional surface cracking both experimentally and theoretically, field excursions to Dangan Island, and earthquake data analysis for Dangan Islands area. All these works are related to shallow earthquakes occurred in the northern part of the South China Sea within 150 km away from Hong Kong. In particular, the foci of a total of 26 small earthquakes recorded by the Hong Kong Observatory from 1998 to 2003 are plotted three-dimensionally, and 3 potential fault zones are identified. It was identified that Haifeng Fault Zone may be related to some of the small shallow earthquakes reported in this area. Much research needs to be done to verify this speculation. Fault zones on Dangan Island are identified after our field excursions to the island, suggesting a series of normal faults trending ESE and NE on the island. To examine the potential future faulting, specimens containing 3-D surface cracks are compressed to examine the cracking pattern. Shell and pedal cracks around the pre-existing three-dimensional surface crack were observed. Vertex singularities at the intersection between the surface crack and the free surface are reviewed and some new approximate formulas are proposed for engineering application. Simple approximate formulas are also proposed for the stress intensity factors of partially circular surface cracks under far field shear stress. The wing crack model proposed by Dyskin et al. (1999) is modified here to predict the growth of wing crack as a function of crack inclination, fracture toughness, and applied stress.

Our experimental and theoretical works suggested that crack or fault branching is very likely to occur during small earthquake occurrence if the pre-existing fault can be modeled as a shallow three-dimensional surface crack. The results of this study provide hints on the mechanism of future continental earthquakes in the northern part of the South China Sea, for which subsurface fault zone may not be fully developed. The faulting information can be used for simulating more reliable seismic ground motions by using stochastic point source method (Liu et al., 2003). As demonstrated by our previous works, the seismic soil-pile-structure interaction (Koo et al., 2003), the seismic pounding between two adjacent buildings (Chau and Wei, 2001; Chau et al., 2003), and seismic vulnerability of building (Wen et al., 2002) are highly sensitive to the magnitude as well as frequency content of the input ground motions. Therefore, the present studies on earthquake mechanics are very important for the estimation of seismic hazard for Hong Kong.

ACKNOWLEGEMENT

The work described in this paper is fully supported by PolyU Project No. A-PF62, by a grant from the Research Grants Council of the Hong Kong Special Administrative Region, China (Project No. PolyU 5136/03E), and by the National Natural Science Foundation of China (Project Nos. 40272120, 50229901). The first author is grateful to Professor Z.P. Bazant of Northwestern University of discussing the issue of surface singularity at surface crack.

REFERENCES

Bazant, Z.P. and Estenssoro, L.F. (1979). Surface singularity and crack propagation. *International Journal of Solids and Structures* **15**, 405-426.

Benthem, J.P. (1977). State of stress at the vertex of a quarter-infinite crack in a half-space. *International Journal of Solids and Structures* **13**, 479-492.

Benthem, J.P. (1980). The quarter-infinite crack in a half space: alternative and additional solutions. *International Journal of Solids and Structures* **16**, 119-130.

Borberg, K.B. (1999). *Cracks and Fracture.* Academic Press, San Diego, USA.

Chau, K.T. and Wei, X.X. (2001). Pounding of structures modeled as nonlinear impacts of two oscillators. *Earthquake Engineering and Structural Dynamics* **30:5**, 633-651.

Chau, K.T., Wei, X.X., Guo, X. and Shen, C.Y. (2003). Experimental and theoretical simulations of seismic pounding between adjacent structures. *Earthquake Engineering and Structural Dynamics* **32:4**, 537-554.

Dyskin, A.V., Germanovich, L.N., Jewell, R.J., Joer, H., Krasinski, J.S., Lee, K.K., Roegiers, J.-C., Sahouryeh, E. and Ustinov, K.B. (1994). Study of 3-d mechanisms of crack growth and interaction in uniaxial compression. *ISRM News Journal* **2:1**, 17-24.

Dyskin, A.V., Germanovich, L.N. and Ustinov, K.B. (1999). A 3-D model of wing crack growth and interaction. *Engineering Fracture Mechanics* **63**: 61-110.

Feng, H. (Ed) (1988). *A Complete Catalogue of Earthquakes in China, 1980.* Seismological Press (in Chinese).

Koo, K.K., Chau, K.T., Yang, X., Lam, S.S. and Wong, Y.L. (2003). Soil-pile-structure interactions under SH waves. *Earthquake Engineering and Structural Dynamics* **32:3**, 395-415.

Lai, K.W. and Langford, R.L. (1996). Spatial and temporal characteristics of major faults of Hong Kong. *Seismicity in Eastern Asia, Geological Society of Hong Kong Bulletin No.* **5**, 72-84.

Lee, C.M. and Workman, D.R. (1996). Earthquakes in the South China region and their impact on Hong Kong. *Seismicity in Eastern Asia, Geological Society of Hong Kong Bulletin No.* **5**, 92-103.

Liu, J, Zheng, S. and Wong, Y.L. (2003). The inversion of anelastic coefficient, source parameters, and site response using genetic algorithm. *Acta Seismologica Sinica* **16:2**, 226-232.

Murakami, Y. (1987). *Stress Intensity Factors Handbook.* Vol. 2, Pergamon, Oxford, UK.

Murakami, Y. and Natsume, H. (2002). Stress singularity at the corner point of 3-D surface crack under mode II loading. *JSME International Journal A-Solid Mechanics* **45:2**, 161-169.

Tada, H., Paris, P.C. and Irwin, G.R. (1985). The *Stress Analysis of Crack Handbook.* St. Louis, Del Research Corporation.

Wen, Z.P., Hu, Y.X. and Chau, K.T. (2002). Site effect on vulnerability of high-rise shear-wall-buildings under near and far field earthquakes. *Soil Dynamics and Earthquake Engineering* **22:9-12**, 1175 – 1182.

Wong, R.H.C., Law, C.M., Chau, K.T. and Zhu, W.S. (2004a). Crack propagation from 3-D surface fractures in PMMA and marble specimens under uniaxial compression. *International Journal of Rock Mechanics and Mining Science* **41:3**, 360 (full paper in CD-ROM).

Wong, R.H.C., Huang, M.L., Jiao, M.R., Tang, C.A. and Zhu, W. (2004b). The mechanisms of crack propagation from surface 3-D fracture under uniaxial compression. *Key Engineering Materials* **261-263**, 219-224.

Xia, K. (1985). The first sea bottom seismometer test in the South China Sea shallow water area. *Proceedings of the Seminar on Marine geology of Hong Kong and the Pearl River Mouth.* Hong Kong Geological Society, HK, 29-37.